Image potential and local field effects on ionization rates in the field ion microscope

1993 J. Phys.: Condens. Matter 5 1833

(http://iopscience.iop.org/0953-8984/5/12/011)

J. Phys.: Condens. Matter 5 (1993) 1833–1840. Printed in the UK

Image potential and local field effects on ionization rates in the field ion microscope

C M C de Castilho, R F S Andrade and C T Sousa
Instituto de Física, Universidade Federal da Bahia, 40210-340 Salvador, Brazil

Received 12 August 1992, in final form 7 December 1992

Abstract. Effects of both the local field and the image potential are taken into account in the determination of the ionization rates of the imaging gas in the field ion microscope. The model consists of a half-sphere superimposed on a flat surface and the results were obtained after the JWKB scheme. In comparison with the more usual cases, where only the external field and the atom potential are considered, the overall effect is to narrow the ionization zone and to decrease the ionization rate, except for the part of the ionization zone closest to the surface.

1. Introduction

The tunnelling of an electron through a potential barrier is the basic phenomenon for image formation in the field ion microscope (Müller and Tsong 1969). This barrier results from the superposition of the several 'components' of the potential experienced by the electron. Among them we may identify two major aspects: the first is due to the atomic nucleus or resulting molecular forces which binds the electron, and the second is related to the external electric field. The basic form of the barrier due to these two 'components' is indicated in figure 1. This picture is a satisfactory representation of the actual situation when the imaging gas molecule is far away from the sample surface of the field ion microscope and is referred to as free-space field ionization (FSFI) (Haydock and Kingham 1981a, de Castilho and Kingham 1986). Close to the surface, additional aspects need to be included in the expression for the potential. They are necessary to explain the process of image formation in the field ion microscope, where brighter zones in the screen correspond to small regions in which the production of ions is increased as the result of a stronger electric field. Two such aspects have been pointed out as being important in modelling the electric field close to the surface: the influence of protrusions on the atomic scale (adatoms, kinks and steps) which are always present; the effect of image charges, which explain the collective rearrangement of free charges within the metal, induced by the presence of the electron and nucleus of the imaging gas molecule close to the surface. Both of these have been recently considered in the literature (de Castilho and Kingham 1986, Lam and Needs 1992, de Castilho 1992). However, until now these effects have been treated independently of each other.

In this work we present a study of the influence of *both* effects in the ionization rates of a gas molecule. The most important point is the determination of the potential which describes this situation. This has been accomplished by modelling a

0953-8984/93/121833+08\$07.50

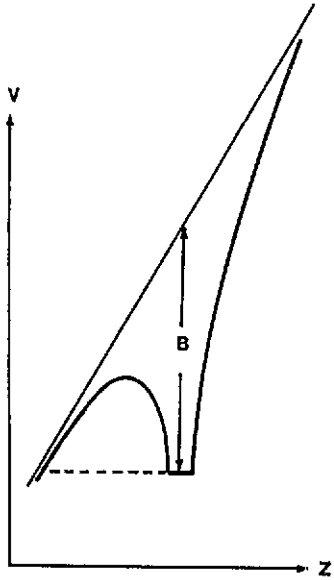

Figure 1. One-electron potential energy in the imaging gas molecule far from the surface. Its main 'components' are the hydrogen-like potential and the external electric field.

flat surface plus one protruding atom by a geometry consisting of the plane plus a half-sphere. For such geometry the position of the image charges can be explicitly given. Once the potential has been obtained, we have used a standard numerical method of calculating the transmission rate across a barrier by the JWKB approximation. As we shall see in the following sections, the introduction of both effects in this problem causes an enhancement of the ionization rates in the very close neighbourhood of the surface. This may be of relevance in the explanation of the image contrast in the field ion microscope.

The rest of the paper is organized as follows: in section 2 we present the basic arguments which lead to our model and point out the positions of the image charges and the resulting potential. In section 3 we indicate the basic steps of the JWKB method and discuss our results. Section 4 closes the paper with concluding remarks.

2. Basic model

2.1. *Electrostatic images to a plane + semisphere*

The usual tips used in field ion microscopy experiments have an apex radius of about 500 Å. Their actual form is not fixed, and several geometric shapes (hyperbolic, parabolic, etc) have been used in the theoretical description of the problem (Müller and Tsong 1969, de Castilho and Kingham 1986). On the other hand, a protrusion consists of one atom or a few atoms, so that the order of magnitude of its radius is about 100 times smaller than that of the overall tip geometry. The effects of the protrusion that we are mainly interested in are the enhancement of the electric field in its neighbourhood and its influence on the ionization rate. Such effects occur very close to the surface in such a way that for their description the tip can be approximated by a plane. Although this simplification looks qualitatively reasonable, it can also be quantitatively justified by the comparison of the ionization distribution for the two geometries; for distances of about 30 Å from the surface and upwards, the ionization rate caused by a smooth hyperbolic surface agrees with that due to a plane, if we consider the same field intensity. If we are interested in the effects of image charges induced by a point charge, this approximation is crucial. We reduce the problem to a highly symmetric geometry consisting of a semisphere (protrusion) superimposed on a plane, which admits an exact solution for the image charges. We also include a screening correction that gives a zero potential along the flat surface plus protrusion.

The solution to the problem of finding the position of the image charges to this geometry follows from the solutions to two classical problems: firstly the point charge plus plane and secondly the point charge plus sphere—which are available in several textbooks (see e.g. Panofsky and Phillips (1962)). The basic situation is sketched in figure 2. For definiteness let us put the origin of our coordinate system at the centre of the sphere of radius a (protrusion), and let the direction z be perpendicular to the plane, while using spherical coordinates (r, θ, ϕ) in the usual way, for a 'right-hand' system of coordinates. First we observe that the physical space where the point charge may be found is limited to $r > a$, $\theta < \pi/2$. If we consider a point charge q at the position (r_1, θ_1, ϕ_1), it is well known that an image charge $-q$ at the point $(r_1, \pi - \theta_1, \phi_1)$ gives a zero potential to the x–y plane. On the other hand, it is also known that a charge $-qa/r_1$ at the point $(a^2/r_1, \theta_1, \phi_1)$ assigns a zero potential to the surface of the sphere. Finally we realize that these two image charges plus a third image charge, whose value is qa/r_1, placed at the point $(a^2/r_1, \pi - \theta_1, \phi_1)$ give a zero potential at both the x–y plane and the 'outer part' of the sphere of radius a.

2.2. *The ionization potential*

To introduce the image charges discussed above into our problem it is necessary to make a more accurate analysis of the situation when the electron tunnels through the potential barrier and approaches the surface. Since the problem is left invariant by the rotation of an angle ϕ about the z axis, we may consider only a two-dimensional (2D) version of it, which amounts to considering ϕ as a constant. The solution for the complete problem can then be obtained by multiplying the 2D result for a constant ϕ by 2π.

We are interested in the motion of the electron due to the atomic nucleus potential, the external field and the image potentials. The first two terms of the electron potential have been considered by de Castilho and Kingham (1986) and have the form

$$V(\rho, \alpha; z) = -F(z)\rho \cos \alpha - Q/\rho. \tag{1}$$

In the above equation, F is the electric field at the point (0, 0, z) where the nucleus is found, ρ is the distance to the electron measured from the nucleus position, α is the angle formed with the negative z direction, and Q is the nucleus charge. According to de Castilho and Kingham (1986), the effect of the protrusion can be described by a field $F(z)$ of the form

$$F(z) = F_0\left[(1 + z/R_T)^{-1} + (a/z)^3\right] \tag{2}$$

for a hyperboloidal tip plus a superimposed sphere, where R_T is the overall tip radius for the hyperboloid. In our case, where the hyperboloidal surface will be approximated by a plane, equation (2) reduces to

$$F(z) = F_0[1 + (a/z)^3]. \tag{3}$$

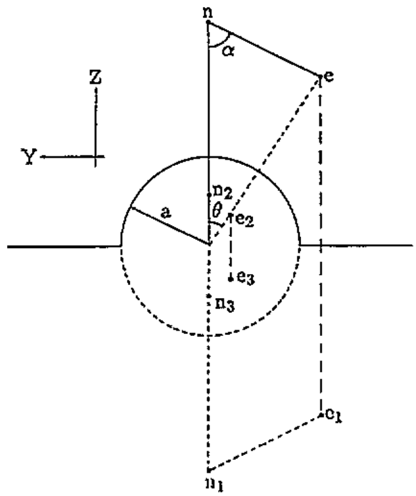

Figure 2. Position of the nucleus n, tunnelling electron e and their image charges n_1, n_2, n_3 and e_1, e_2, e_3.

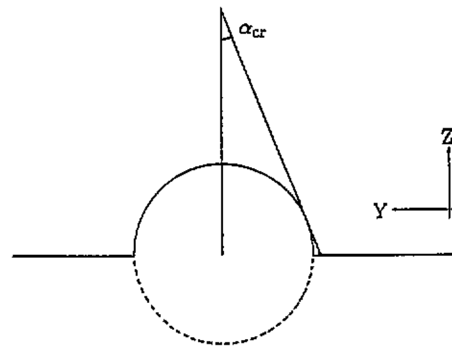

Figure 3. Illustration of the critical angle α_{cr} for an electron tunnelling from an atom at the point z. At this point the 'trajectory' is a tangent to the protrusion.

As discussed above, there are three image terms for each actual charge (electron and nucleus). Moreover we observe that in the ionization process the nucleus is assumed to be static whereas the electron moves through the potential barrier to reach the surface. It follows that the image charges of the nucleus stay far away from the surface, but those of the electron approach the electron itself when it collapses into the surface. This would lead to a divergence in the expression for the electrostatic potential energy. To side step this unphysical effect it is necessary to remove this divergence, introducing a screening factor whose major effect is to keep bounded the interaction energy (in fact, equal to the work function) when the electron reaches the surface. This procedure has also been adopted by Lam and Needs (1992). So, if we suppose that the nucleus stays in the direction on top of the protrusion ($\alpha = 0$), the image potentials of the nucleus and electron are respectively given by (figure 2):

$$V_{\text{in}} = Q\Big\{\left[4z^2 - 4z\rho x + \rho^2\right]^{-1/2} + (a/z)\left[(z - a^2/z)^2 - 2(z - a^2/z)\rho x + \rho^2\right]^{-1/2} - (a/z)\left[(z + a^2/z)^2 - 2(z + a^2/z)\rho x + \rho^2\right]^{-1/2}\Big\} \tag{4}$$

$$V_{\text{ie}} = -\Big[\tfrac{1}{4}(z^2 - 2z\rho x + \rho^2 x^2)^{-1/2} - (a/2)(z^2 - 2z\rho x + \rho^2 + a^2)^{-1} + (a/2)\Big(\big[\!\big[- \exp\{-4\Phi[(z^2 - 2z\rho x + \rho^2)^{1/2} - a]\}\big]\!\big] \times (z^2 - 2z\rho x + \rho^2 - a^2)^{-1}\Big)\Big] \tag{5a}$$

$$V_{\text{ie}} = -\big[\!\big[\tfrac{1}{4}\{1 - \exp[-4\Phi(z^2 - 2z\rho x + \rho^2)^{1/2}]\}/(z^2 - 2z\rho x + \rho^2)^{1/2} - (a/2)(z^2 - 2z\rho x + \rho^2 + a^2)^{-1} + (a/2)(z^2 - 2z\rho x + \rho^2 - a^2)^{-1}\big]\!\big] \tag{5b}$$

where $x = \cos\alpha$ and Φ is the work function. The potential of the electron image charges is given by two different expressions since the screening will be different, depending on whether the electron approaches the surface on top of the protrusion ($\alpha < \alpha_{cr}$, equation (5*a*)) or towards the plane ($\alpha > \alpha_{cr}$, equation (5*b*)), as can be seen in figure 3. The value of α_{cr} is given by

$$\tan\alpha_{cr} = \pm a/\sqrt{z^2 - a^2}. \tag{6}$$

This results from the condition that the trajectory of an electron tunnelling from the atom at the point z to the surface along this direction will be 'tangential' to the protrusion.

3. Ionization rates

The JWKB approach is adequate for the evaluation of the ionization probability per unit of time (ionization rate) for a molecule (atom) placed in a certain position z and can be expressed, in one dimension, by

$$R(z) = A^2 \exp\left(-2^{2/3} \int_{\rho_0}^{\rho_1} (V(\rho; z) - E)^{1/2}\, \mathrm{d}\rho\right) \tag{7}$$

where ρ_0 and ρ_1 are the internal and external classical turning points, $V(\rho; z)$ is the particle potential, E is the energy of the particle and A is a constant factor. An extension of equation (7), conceived in order to simulate a 3D calculation, was proposed by Haydock and Kingham (1981b) and has the form

$$R(z) = A^2 \int_{\alpha=0}^{\alpha_m} \int_{\phi=0}^{\phi_m} \exp\left(-2^{3/2} \int_{z_0(\alpha,\phi)}^{z_1(\alpha,\phi)} [V(\rho; z) - E]^{1/2}\, \mathrm{d}\rho\right) \sin\alpha\, \mathrm{d}\alpha\, \mathrm{d}\phi. \tag{8}$$

Here the classical turning points depend on the 'tunnelling direction' (α, ϕ), so that the integration in α and ϕ corresponds to a 'sum' over the solid angle.

Both ionization rates given above are calculated assuming that the tunnelling particle is available for the process, i.e. an image gas molecule does exist at point z. This stays in contrast with the actual simulation in the field ion microscope, where the gas molecule moving towards the surface can, in principle, be ionized at any point of its trajectory. This means that such an ionization rate is not suitable for direct comparison with experimental data (de Castilho 1992). However, using the expression of the ionization rate for a molecule approaching the sample from a distant point we can define the survival probability of a molecule, i.e. the probability that it is not being ionized. This leads to an ionization probability at the point z which takes into account its 'history' on the way towards the surface (Haydock and Kingham 1981b, de Castilho and Kingham 1986) and can be expressed by

$$D(z) = R(z) \exp\left(-\int_z^{\infty} R(z')\, \mathrm{d}z'\right). \tag{9}$$

This is the basic quantity for the comparison between theoretical curves and experimental data of the ionization distribution as a function of position or, alternatively, electrostatic energy deficit (de Castilho 1992). In what follows we shall present our results of the 3D ionization rate per unit distance, which is simply the

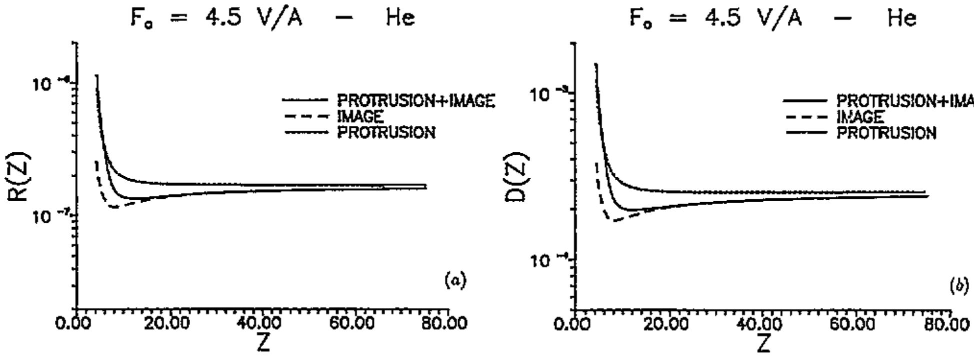

Figure 4. (*a*) Ionization rate per unit time and (*b*) ionization distribution as functions of the position where we consider, separately, the local enhancement of the electron field (protrusion) and the image effect. The combined effect is also shown.

ionization rate divided by the velocity of the molecule at that point, and the ionization probability $D(z)$ considering the chance of survival.

We have evaluated both $R(z)$ and $D(z)$ for several values of the external applied field. The imaging gas was considered to be helium, and the integration over the solid angle, as indicated in equation (8), was performed by taking $\phi_m = 360°$ and $\alpha_m \simeq 53°$. This value for ϕ_m follows from the already-mentioned symmetry of the model regarding the azimuthal component, whereas it is known that for $\alpha > \alpha_m$ the individual contribution of equation (7) is negligible. We show in figure 4 some of the typical curves that we have obtained. There we represent the ionization rate $R(z)$ and ionization distribution $D(z)$ showing the effects due to the local electric field and due to the image charges, and the 'combined effect'. To discuss our results we should describe what happens when we separately include the contributions of local field and image charges in the free-space situation, where only the external field and nuclear potential $1/r$ are taken into account. de Castilho and Kingham (1986) have shown that the local field causes the enhancement of the ionization rate, for distances up to at most 50 Å from the surface. For larger distances the local field loses any influence on the ionization rate. On the other hand, Lam and Needs (1992) indicate that the presence of image charges in a flat surface causes a reduction in the ionization rate. The analysis of our figures show that the global effect of these contributions is to reduce the ionization rate when the atom is at intermediate distances (10–40 Å) from the surface, but in the immediate vicinity of it we observe that the ionization rate increases sharply and exceeds the ionization rate when no image charge is present. This can be regarded as the main result of this work, since it is an indication that the ionization will be more localized, occurring in the very close neighbourhood of the surface, in accordance with very well established experimental observations (Müller and Tsong 1969). On the other hand, this narrow localization of the ionization zone is important to explain the image contrast in the field ion microscope (Forbes 1985, de Castilho and Kingham 1986). As can be easily seen, the full curve corresponding to the combined effect of the local field enhancement and image charges, at distances close to the critical distance, becomes higher if we compare it with the two other curves.

In figure 5 we show the ionization distribution as a function of distance for different values of the 'overall' electric field. It is possible to observe the presence of

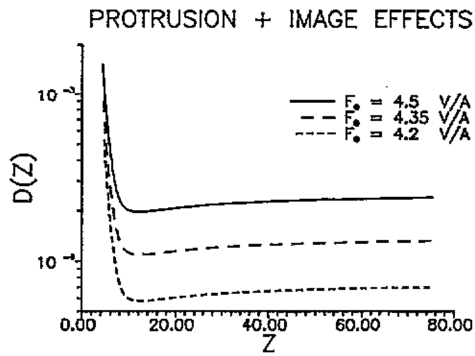

Figure 5. Ionization distribution $D(z)$ as a function of the position for different values of the 'overall' tip field.

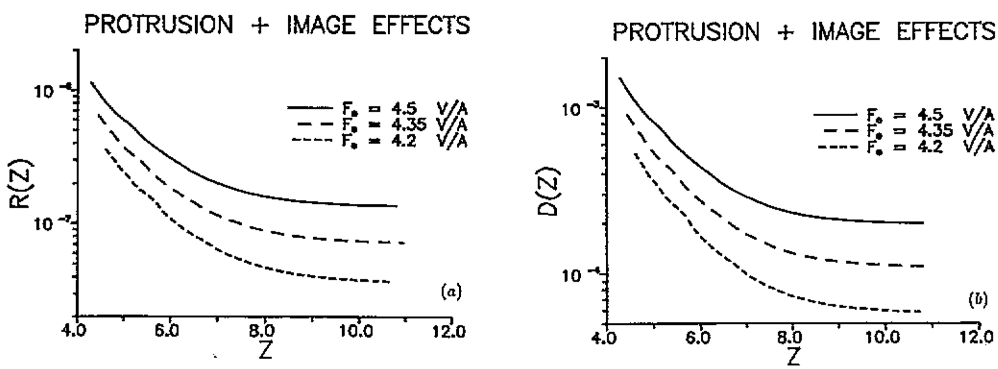

Figure 6. Details of the curves shown in figure 4 (combined effect) in the very close neighbourhood of the surface, for different values of the tip field.

some structure in the ionization rate curves for very short distances from the surface, whereas the case without image charges has a very smooth curve. It is essential to distinguish here the kind of structure in the curve reported here from previous work in the literature (Jason *et al* 1965, de Castilho and Kingham 1986, de Castilho 1992). The former (Jason effect) results from resonant effects not included in this work. The latter structure, reported by de Castilho and Kingham (1986) and de Castilho (1992), is related to the ionization distribution and *not* to the ionization rates, where their calculated curves are absolutely smooth. On the other hand, the structure observed here (figure 6) appears in the ionization rate curves (figure 6(a)) and also in the ionization distribution curves (figure 6(b)). Peaks of this kind have been referred to not only as the 'Jason (1967) peaks' but also as resulting from surface plasmons (Lucas 1971), although the last possibility has been largely discredited. What is relevant is the possibility that these peaks appear here in a very natural way from the combined effects of the image charges, local field enhancement and an integration effect from $R(z)$ to $D(z)$, as pointed out by de Castilho and Kingham (1986). In the present case, their origin can be followed by noting that the reduction in the value of α_m implies that the contributions that we take into account are due to tunnelling paths concentrated around the half-sphere. This structure can be seen more clearly in the case of H_2 as the imaging gas, provided that we restrict the limit of integration in the α variable. For instance, when we take $\alpha_m \simeq 11.5°$, we see in figure 7 that the small structures observed for He in figure 6 are largely enhanced, combining to give a single sharp peak, also very close to the surface. So it becomes clear that the occurrence of the structure is certainly due to the presence of the local field contribution together with the image charge potential that it introduces in the problem. The structure then is not introduced by any artefact of the model. More realistic values for α_m reduce significantly this 'peak', so figure 7 is included only to demonstrate our reason for interpreting the origin of this kind of 'structure'.

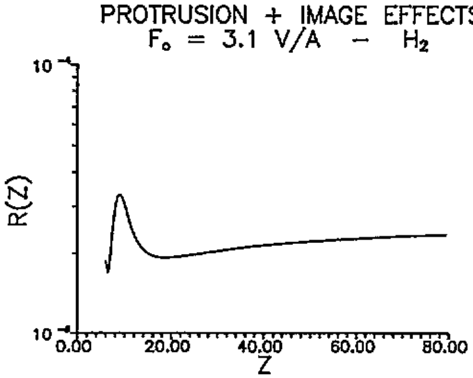

Figure 7. Curves of $D(z)$ for the imaging gas H_2, when the integration of equation (8) is restricted to $\alpha_m \simeq 11.5°$.

4. Conclusions

We have shown that the physical model for the potential barrier to be tunnelled by an electron when the ionization process takes place very close to the sample must include effects of image charges and local electric field enhancement, besides the usual external field and nucleus potential which are sufficient for FSFI. We have been able to include simultaneously both effects by using six image charges (three associated with the tunnelling electron and three with the nucleus charge) and an *ad hoc* expression for the electric field simulating a local protrusion. This has led to some structure not only in the distribution curve $D(z)$ but also in the ionization rate curves. As previously pointed out by Lam and Needs (1992), the inclusion of the image potential causes a minimum in such curves. Our work, however, shows the combined effect of the image potential plus the local enhancement of the electric field, giving even higher values for the ionization rate at or very close to the critical distance. This, we strongly believe, can lead to a better theoretical determination of the ionization zone width.

References

de Castilho C M C 1992 *J. Phys.: Condens. Matter* **4** 1039–46
de Castilho C M C and Kingham D K 1986 *Surf. Sci.* **173** 75–96
Forbes R 1985 *J. Phys. D: Appl. Phys.* **18** 973–1018
Haydock R and Kingham D R 1981a *J. Phys. B: At. Mol. Phys.* **14** 385–96
—— 1981b *Surf. Sci.* **103** 239–47
Jason A J 1967 *Phys. Rev.* **156** 266–85
Jason A J, Burns P B and Inghram M G 1965 *J. Chem. Phys.* **43** 3762–3
Lam S C and Needs R J 1992 *Surf. Sci.* at press
Lucas A A 1971 *Phys. Rev. Lett.* **26** 813–6
Müller E W and Tsong T T 1969 *Field Ion Microscope: Principles and Applications* (Amsterdam: Elsevier)
Panofsky W K H and Phillips M 1962 *Classical Electricity and Magnetism* (Reading, MA: Addison-Wesley)